J. health med. sci.,
9(3):11-16, 2023.

Assessment of image quality in digital radiology using the CDRAD contrast-detail phantom in pediatrics

Evaluación de la calidad de la imagen en radiología digital utilizando el fantoma de detalle de contraste CDRAD en pediatría

Priscila Resmer Castilho[1]*, Hugo Schelin[1], Valeriy Denyak[2, 3], Rosiane Mello[1], Adriano Legnani[1], Sergei Paschuk[2, 3]

RESMER, P.; SCHELIN, H.; DENYAK, V.; MELLO, R.; LEGNANI, A.; PASCHUK, S. Assessment of image quality in digital radiology using the CDRAD contrast-detail phantom in pediatrics. *J. health med. sci., 9(3)*:11-16, 2023.

ABSTRACT: The transition from analog to digital radiology has expanded the capabilities of radiological imaging but has also made it possible to increase the radiation dose received by patients. Image quality in radiology is determined by factors such as radiographic techniques (kVp and mAs), which directly impact the dose and image quality. This study focuses on pediatric radiological exams considering their greater radiosensitivity and longer life expectancy. The study aimed to investigate the correlation between image quality and applied radiographic techniques using the CDRAD contrast-detail phantom. The results showed a direct linear relationship between the increase in kVp and the corresponding increase in image quality. Nonetheless, there was a significant variation in image quality between current-time products ranging from 0.5 to 2.5 mAs, in contrast to the nearly linear relationship observed within the 2.5 and 10 mAs range.

KEYWORDS: contrast-detail, CDRAD, digital radiology, pediatrics.

INTRODUCTION

Radiographic image quality pertains to the defined ability to visualize and differentiate nearby structures. Within digital radiology, spatial resolution, and contrast resolution hold paramount importance. Distinct visual representations arise when densities alter with consistent thickness. Similarly, when density remains constant while minimal thickness changes, this distinction should manifest in the resulting image. Sufficient contrast is essential for detecting such disparities. The contrast-detail curve serves as a method for assessing both types of resolution (Al-Murshedi *et al.*, 2018).

Image quality not only impacts clinical diagnosis but also plays a crucial role in the potential reduction of radiation dose during radiological examinations (Piantini *et al.*, 2017). Therefore, it is essential to establish dose thresholds that ensure the use of the minimum radiation dose is feasible (Al-Murshedi, *et al.*, 2019; GHARAREHAGHAJI *et al.*, 2019). The irradiation dose administered depends on the specific radiographic techniques employed, such as kilovoltage peak (kVp) and current-time product - milliamperes per second (mAs), which subsequently influence the resulting image quality (GOIS *et al.*, 2019; Alresheedi N., *et al.*, 2021).

This phenomenon arises because voltage contributes to the establishment of the optimal gray-scale, as it possesses sufficient energy to penetrate a structure of specific thickness, accounting for the relative proportions of bone, air, and soft tissues. The mAs setting adjusts the technique to yield an image with optimal contrast resolution, factoring in the quantity and duration of irradiation. In the Konst *et al.*, (2019) study assert that achieving diagnostic quality necessitates the discernment of low-contrast structures, technically referred to as image intensity resolution. Furthermore, it is feasible to define the minimum radiation dose required to achieve satisfactory detail and image quality for diagnostic purposes by detect-

1 Faculdades Pequeno Príncipe, Instituto de Pesquisa Pelé Pequeno Príncipe, Curitiba, PR, Brazil.
2 Federal University of Technology - Paraná, Curitiba, PR, Brazil.
3 National Science Center “Kharkov Institute of Physics and Technology”, Kharkiv, Ukraine.
* E-mail: priresmer@gmail.com

ing these low-contrast structures. Among the various approaches to validate and enhance studies in digital radiology, particularly in the evaluation of low-contrast structures, the utilization of a contrast-detail phantom stands out (Al-Murshedi *et al.*, 2018).

This study investigates the relationship between image quality and applied radiographic techniques. Due to the importance of these protocols in pediatric settings, where children are particularly sensitive to radiation, the research was conducted in an exclusively pediatric hospital in Curitiba (Brazil). The phantom contrast-detail CDRAD (Artinis Company) acquired images using different radiographic techniques to study their impact on image quality.

MATERIALS AND METHODS

The measurements were conducted using a Shimadzu Flexavision equipment, following standardized protocols for pediatric chest imaging. To determine the technical parameters of voltage (kVp) and current product-time (mAs), a survey was conducted based on studies by (Piantini *et al.*, 2017). Voltage variations ranging from 70 and 83 kVp were utilized. Five polymethylmethacrylate (PMMA) plates, each measuring 1 cm, were employed. The contrast-detail phantom CDRAD was positioned beneath the plates, as depicted in Figure 1.

This phantom is composed of an acrylic plate, with holes in diameters ranging from 0.3 to 8 mm ± 0.03 mm (Burght *et al.* 2017). Each row of holes corresponds to a specific column with holes of the same size but varying depths. In the image obtained through irradiation, a specialized software detects the number of visible holes, enabling the creation of a contrast-detail curve (Konst *et al.* 2019).

The positioning of the PMMA plates and the CDRAD phantom remained unchanged throughout the irradiation process. Measurements were conducted at 1.1 m from the focal point to the detector. The reproducibility test was performed using the 70 kVp and 2 mAs technique, where three consecutive images were captured with the same technique. It was performed by reproducing 3 simultaneous images one after another, with the same technique, sequentially. Furthermore, voltage variation tests were performed at 70 kVp, 75 kVp, and 80 kVp, with a current of 1 mAs. The current-time product was varied between 0.5 mAs, 2.5 mAs, 5 mAs, and 10 mAs while maintaining a voltage of 83 kVp.

Following image acquisition, the images were analyzed utilizing the CDRAD Analyzer 2.1.15 software. The Alpha parameter was set to 10^{-8}, and the “Multivariable contrast detail curve” function was employed for the analysis.

The contrast-detail curve is shown in Figure 2, where the hole depth is plotted against the corresponding hole diameter. In the multivariable contrast-detail curve, the contrast (line C), the detail (line D), and the combined assessment (line CD) is determined using equation (1) (Burght *et al.* 2017):

$$f(x,y) = \frac{3}{3 + e^{f(x-a)} + e^{g(y-b)} + e^{h(x\cos(\alpha)+y\,sin(\alpha)-c)}} \qquad (1)$$

Where:

Figure 1. Arrangement of the CDRAD phantom and the PMMA plates.
Source: Own authorship, 2022.

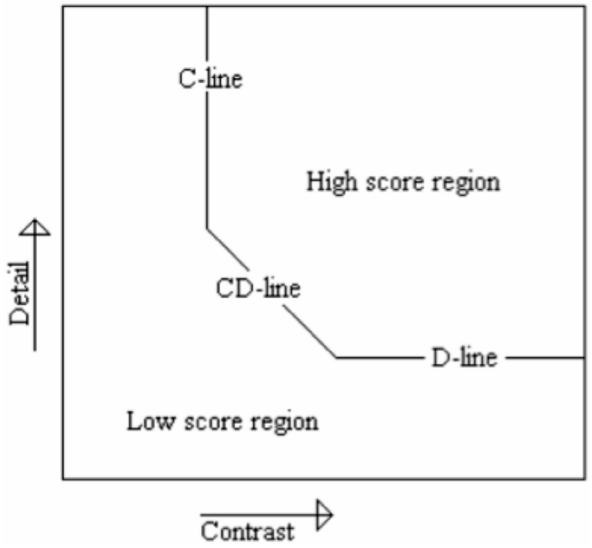

Figure 2. Illustrative image adapted from the Artinis Manual, showcasing the representation of the multivariable contrast-detail curve.
Source: Artinis Manual (Burght *et al.*, 2017).

- f (x, y) denotes the CD curve;
- a corresponds to the position of line C;
- b represents the location of line D;
- c denotes the interception of the CD line on the y-axis;
- f, g, and h represent the slopes of the transitions from top to bottom for lines: C, D, and CD, respectively;
- α represents the angle of the line CD concerning the axis.

Image quality can be assessed by the number of accurately identified holes relative to the total number of squares, where a higher value signifies a better image quality. Another method for calculating image quality is using the Image Quality Figure method, IQF, defined by equation (2) (Burght *et al.* 2017).

$$IQF = \sum_{i=1}^{15} C_i \cdot D_{i,th} \qquad (2)$$

In the equation:

- C_i represents the contrast value for each column.
- $D_{i,th}$ corresponds to the threshold diameter (th) in the contrast column C_i.

The sum of all contrast columns yields the IQF (Image Quality Figure). For completely invisible columns, the $D_{i,th}$ is set to 10 mm, while for completely visible columns, the $D_{i,th}$ value is 0.3 mm. These values consider the hole depth ranging from 0.3- and 8-mm. Since the IQF decreases as the diameter values and the depth of threshold holes decrease, the inverted IQF approach (IQF_{inv}) is employed, as demonstrated in equation (3) (BURGHT *et al.* 2017):

$$IQF_{inv} = \frac{100}{\sum_{i=1}^{15} C_i \cdot D_{i,th}} \qquad (3)$$

The results were then analyzed considering the IQF_{inv} and the percentage of detectability for the applied variations in the parameters of current-time and voltage. These values were determined by multiplying the standard deviation by the Student coefficient for 3 measurements, assuming a Gaussian distribution.

RESULTS

All collected data were acquired with three measurements performed simultaneously and were

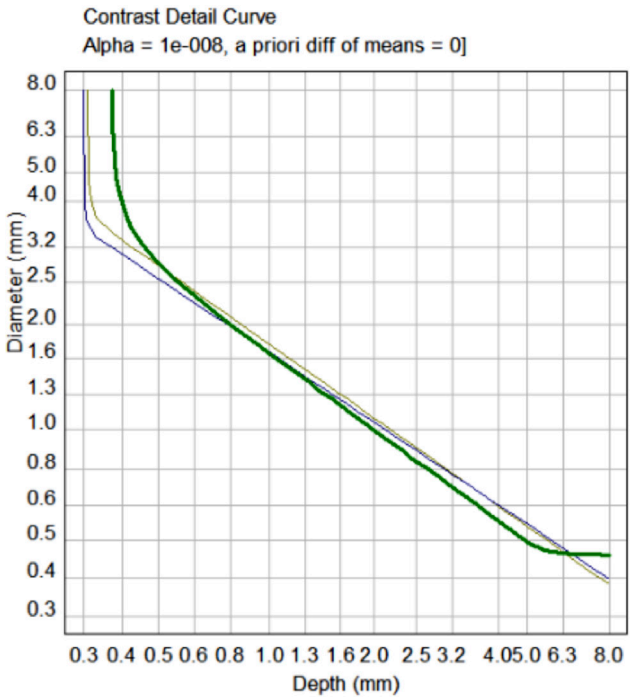

Figure 3. Contrast-detail curve obtained for the reproducibility test for 70 kVp e 2 mAs, generated using the CDRAD Analyzer 2.1.15 software.
Source: Artinis Manual (BURGHT *et al.* 2017).

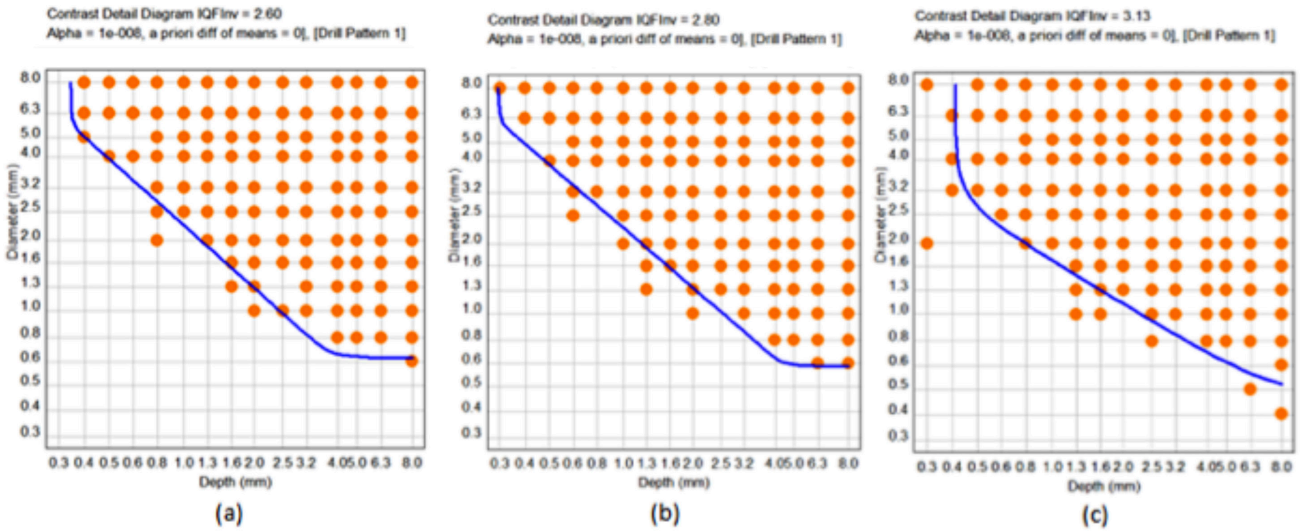

Figure 4. Contrast-detail curves corresponding to the techniques employed: (a) 70kVp and 1 mAs, (b) 75 kVp and 1 mAs, and (c) 80kVp and 1 mAs.
Source: Software CDRAD Artinis 2.1.15

subsequently analyzed utilizing the corresponding contrast-detail curve presented in Figure 3. These measurements allowed for calculating the mean and standard deviation for each analyzed value. Subsequently, comparative analyses were conducted to investigate variations while maintaining the same current but altering the voltage settings. This can be observed in Figure 4, which depicts the variation in the contrast-detail curve resulting from these voltage adjustments to 70, 75 and 80 kVp and the same 1mAs. Table 1 presents, for the same voltage of 83 kVp, the analysis of the different current-time products analyzed in the average IQF_{inv} and the percentage of detectability of the CDRAD phantom points. Figure 5 shows the contrast-detail curve plot for this test. Lastly, an example of the analysis between the IQF_{inv} points can be seen for the current-time product in Figure 6.

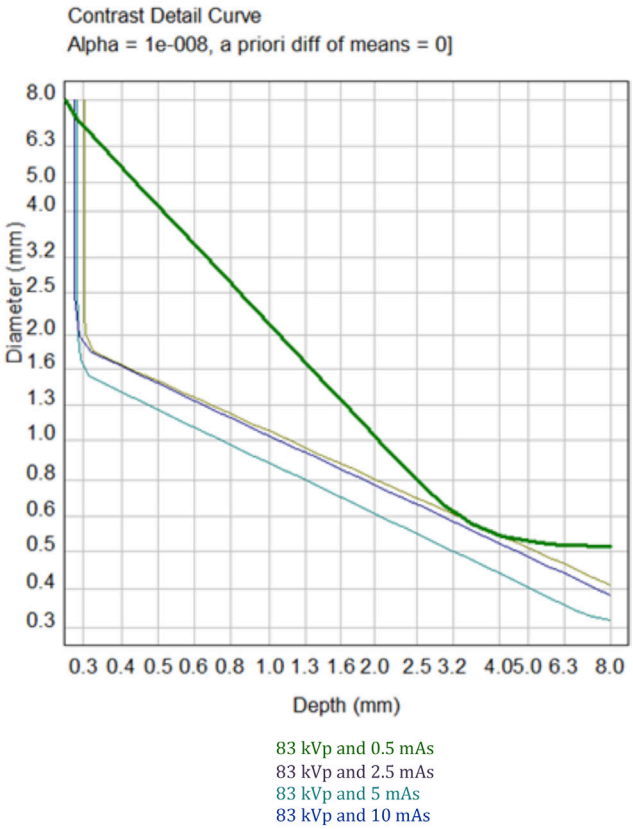

Figure 5. Contrast-detail graph obtained using the CDRAD Artinis 2.1.15 software for the voltage set at 83 kVp and the variation of the current-time product to: 0.5 mAs, 2.5 mAs, 5 mAs and 10 mAs.
Source: Software CDRAD Artinis 2.1.15

DISCUSSIONS

For the reproducibility test, conducted with the parameters of 70 kVp and 2 mAs, yielded IQF_{inv} values of 3.33, 3.42 and 3.57. The total detection rates achieved were 57.78%, 57.78% and 59.11%, respectively. The reproducibility test enabled the calculation of errors, which are reported as 0.16 for the IQF_{inv} and 1.0% for the total detected. Previous studies, such as the research conducted by AL-MURSHEDI, *et al.*, (2019), which investigated the IQF_{inv} average using low-dose techniques across 17 dis-

Table I. Variation in the current-time product at a fixed voltage of 83 kVp.

Current product-time (mAs)	IQF_{inv}	Total detected (%)
0.5	2.49	48.00
2.5	4.57	68.00
5	4.82	69.33
10	4.90	70.22

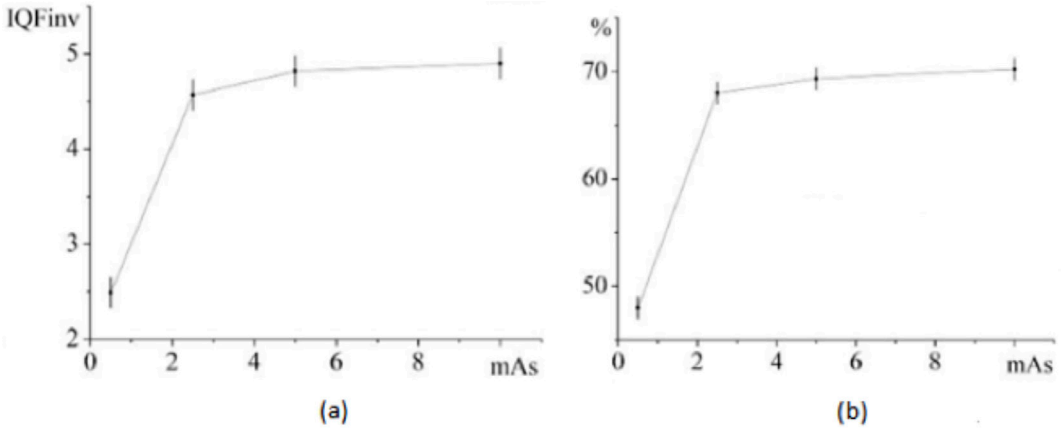

Figure 6. Resulting graphs from the current-time product variation test. In (a), the fluctuations of the mAs values are depicted in relation to the IQF_{inv}, and in (b) the total number of detected points (%). Source: Own authorship, 2022.

tinct pieces of equipment among hospitals, revealed values ranging from 0.87 to 4.73. These values were obtained across four distinct neonatal age groups, with an age range spanning from neonates up to 10 years old (Al-Murshedi, *et al.*, 2019). Table I demonstrates that as the current-time product increases, the IQF_{inv} also increases from 2.49 to 4.90.

In the voltage variation test, the same current-time product of 1 mAs was used for voltages of 70 kVp, 75 kVp, and 80 kVp. The corresponding IQF_{inv} were found to be 2.60, 2.80 and 3.13, respectively. The current-time product variation test was conducted using a voltage of 83 kVp and a current of 0.5 mAs, 2.5 mAs, 5 mAs, and 10 mAs. Additionally, the detection percentage also rises from 48.00% to 70.22%. The voltage variation test demonstrated a linear increase in image quality as the kVp was increased. On the other hand, the current-time product variation test revealed a significant variation between 0.5 mAs to 2.5 mAs, while exhibiting nearly linear behavior between 2.5 and 10 mAs, as depicted in Figure 6. Consistent with these findings, research such as that by Hou, L.-X. *et al.* (2011) suggests that optimizing parameters could significantly reduce radiation doses while having minimal impact on image quality. And other studies report the importance of further studies and relationships with the phantom CDRAD (Geso, M., 2017; Gharareghaghaji *et al.*, 2019; Yalcin, A. *et al.*, 2020).

CONCLUSIONS

The examination of the contrast curve reveals regions of linearity in the current-time product for the 2.5 - 10 mAs interval. This observation implies that, beyond a certain threshold, this technical parameter tends to exert a greater influence on dose rather than on image quality. The established threshold, the dose of exposures, and the dose-IQF ratio collectively propose the need for additional measurements in future research.

ACKNOWLEDGMENT

This study was financed in part by the Coordenação de Aperfeiçoamento de Pessoal de Ní-

vel Superior - Brasil (CAPES) - Finance Code 001, Conselho Nacional de Desenvolvimento Científico e Tecnológico (CNPq), Comissão de Energia Nuclear (CNEN) and Fundação Araucária de Apoio ao Desenvolvimento Científico e Tecnológico do Paraná (FA). We are thankful for the Artinis support by Roeland van der Burght.

RESUMEN: La transición de la radiología analógica a la digital ha ampliado las capacidades de las imágenes radiológicas, pero ha también permitió aumentar la dosis de radiación que reciben los pacientes. La calidad de la imagen en radiología está determinada por factores como las técnicas radiográficas (kVp y mAs), que impactan directamente en la dosis y la calidad de la imagen. Este estudio se centra en exámenes radiológicos pediátricos considerando su mayor radiosensibilidad y mayor esperanza de vida. El estudio está dirigido a investigar la correlación entre la calidad de la imagen y las técnicas radiográficas aplicadas utilizando el detalle de contraste CDRAD fantasma. Los resultados mostraron una relación lineal directa entre el aumento de kVp y el correspondiente aumento de calidad de la imagen. No obstante, hubo una variación significativa en la calidad de la imagen entre los productos actuales que van desde 0,5 a 2,5 mAs, en contraste con la relación casi lineal observada dentro del rango de 2,5 y 10 mAs.

PALABRAS CLAVE: detalle de contraste, CDRAD, radiología digital, pediatría.

REFERENCES

Al-Murshedi, S.; Hogg, P. & England, A. An investigation into the validity of utilizing the CDRAD 2.0 phantom for optimization studies in digital radiography. *British Journal of Radiology*, *91* (1089), 2018.

Al-Murshedi, S.; Hogg, P.; Meijer, A.; Erenstein, H.; England, A. Comparative analysis of radiation dose and low contras.t detail detectability using routine pediatric chest radiography protocols. *European Journal of Radiology***,** 113:198-203*,* 2019.

Alresheedi, N.; Walton, L.; Hogg, P.; Webb, J.; Tootell, A. Evaluation of X-ray table mattresses for radiation attenuation and impact on image quality. *Radiography*, v. 27, p. 215-220, 2021.

Gharehaghaji, N.; Khezerloo, D.; Abbasiazar, T. Image quality assessment of the digital radiography units in Tabriz, Iran: A phantom study. *Journal of Medical Signals and Sensors*, v. 9, n. 2, p. 137-142, 2019

Gois, M.L.C.; Schelin, H.R.; Denyak, V.; Bunick, A.P.; Ledesma, J.A.; Paschuk, S.A. Human factor in exposure from conventional radiographic examinations in very and extremely low birth weight patients. *Radiation Physics and Chemistry*, 155, 31-37, 2019.

Geso, M.; Alghamdi, S.S.; Shanahan, M.; Alghamdi, S.; Mineo, R.; Aldhafery, B. Information Loss Via Visual Assessment of Radiologic Images Using Modified Version of the Low-Contrast Detailed Phantom at Direct DR System. *Journal of Medical Imaging and Radiation Sciences*, 48, 137-143, 2017.

Hou, L., Xie, J., Wang, P. Tang, F. Optimization of image process parameters of digital radiography. *China Journal Radiology*, 2011.

Konst, B.; Weedon-Fekjær, H.; Båth, M. Image quality and radiation dose in planar imaging - Image quality figure of merits from the CDRAD phantom. *Journal of Applied Clinical Medical Physics*, v. 20, n. 7, 2019.

Piantini, F.; Schelin, H.R.; Denyak, V.; Bunick, A.P.; Legnani, A.; Ledesma, J.A.; Filipov, D.; Paschuk, S.A. Dose evaluation in pediatric patients undergoing chest X-ray examinations. *Radiation Physics and Chemistry*, 140, 283-289, 2017.

Burght, R.; Floor, M.; Thijssen, M.; Bijkerk, R. *Manual CDRAD 2.0 Phantom & Analyser software*. [S.l.]: Artinis Medical Systems, v. 2.1, 2017. p. 42.

Yalcin, A; Olgar, T.; Sancak, T.; Atac, G.K; Akyar, A. Correlation between physical measurements and observer evaluations of image quality in digital chest radiography. *Medical Physics*, v. 47, n. 9, 2020.

Autor de Correspondencia
Priscila Resmer Castilho
Faculdades Pequeno Príncipe
E-mail: priresmer@gmail.com

Recibido: 16 de Agosto, 2023
Aceptado: 08 de Septiembre, 2023